

# The frictional behavior of UHMWPE films with different surface energies at low normal loads

Myo Minn and Sujeet K. Sinha

Department of Mechanical Engineering, National University of Singapore, 9 Engineering Drive 1, Singapore 117576, Singapore  
e-mail: [mpesks@nus.edu.sg](mailto:mpesks@nus.edu.sg)

DOI: 10.1016/j.wear.2009.12.032

Publication date (web): 23/December/2009

---

## Abstract

- 1 Introduction
- 2 Experiment procedures
- 3 Results and discussion
- 4 Conclusion

## Acknowledgments

## References

### Abstract

The relationship between initial coefficient of friction,  $\mu_i$  and surface energy (or attractive force) for ultrahigh molecular weight polyethylene (UHMWPE) film is modeled and experimentally measured at low normal loads (15–75 mN). The results show that the initial coefficient of friction increases exponentially with increasing attractive force between a silicon nitride ball and visco-elastic soft UHMWPE film. There is a strong influence of the normal load on this relationship for the polymer surface in the above-mentioned load range. The magnitude of the initial coefficient of friction decreases for UHMWPE film in the higher normal load regime because of its visco-elastic and soft nature as earlier proposed by Bowden and Tabor.

## 1 Introduction

Friction is a major factor that influences the capability and lifespan of machine components. It was earlier believed that friction was only controlled by the geometry of the asperities of the surfaces involved. The Amonton's Laws state that friction is directly proportion to the applied normal loads. However, it was observed later that if two surfaces adhere to each other at rest, there is a finite value of friction even at zero externally applied load [1]. That means, friction is decided by not only the geometry of the asperities but also the surface energy or adhesion force of the surfaces. In fact JKR [2] and DMT [3] models have shown that the contact radius in static condition between solids deviates from the calculated one using the classical Hertzian contact when surface energy is taken into account. Israelachvili and Tabor [4] experimentally measured the contact radius with adhesion effect. Both theoretical and experimental results proved that the role of surface energy on friction is not negligible especially when the applied load is very small.

Yoshizawa et al. [5] studied the correlation between friction and adhesion by means of adhesion energy hysteresis measured in static loading-unloading for polymeric surfaces using the surface force apparatus. Recently, Corwin and de Boer [6] also studied the effect of adhesion on friction in micromachining. In order to reduce the adhesion, monolayer thick lubricants (usually polymers) are applied on surfaces of the devices [7]. The frictional behavior of polymers in terms of adhesion is well studied [8-11]. In liquid films, the surface energy changes also with the thickness of a liquid film. It has been shown that, above a critical thickness, though surface energy normally decreases [12], the static friction increases sharply because of the presence of additional meniscus forces between surfaces [13, 14]. Hence, the effect of meniscus should not be ignored for liquid film or in high humidity environment in low load ranges. The primary focus in many of the current studies has been placed on the interrelation between the surface energy or adhesion and the static friction of polymer and other solids.

The objective of the current paper is to study the initial frictional behavior of soft/visco-elastic UHMWPE film with different surface energies of both the film and the counterface silicon nitride ( $\text{Si}_3\text{N}_4$ ) ball. An analytical relationship between friction and surface energy for UHMWPE film is presented and compared with the current experimental data. The effect of the applied load on the initial coefficient of friction of UHMWPE film is also studied. The initial friction in the present context is defined as the maximum friction force attained at the start of a sliding test.

## 2 Experimental procedures

### 2.1 Materials and sample preparations

Polished n-type silicon (100) wafer of approximately 455-575  $\mu\text{m}$  in thickness was used as the substrate. The UHMWPE solution was prepared by dissolving UHMWPE powder in decahydronaphthalin (decalin) solvent at a temperature of 150  $^\circ\text{C}$  for half an hour and 250  $^\circ\text{C}$  for the next half an hour. A magnetic stirrer was used to speed up the dissolution rate. The UHMWPE film was then coated onto Si substrate by the simple dip-coating method with a dipping and withdrawal speeds of 2.4 mm/s and a dipping duration of 30 s. After that, the coated samples were given heat treatment in a clean air oven at 100  $^\circ\text{C}$  for 15 h. Finally, the samples were cooled down to room temperature in the same clean oven. The thickness of UHMWPE film was approximately 12  $\mu\text{m}$ .

**Table 1.** Surface tension component and parameters of distilled water, ethylene glycol, methanol and hexadecane in  $\text{mJ}/\text{m}^2$  [16].

Liquid	$\gamma_L^{\text{LW}}$	$\gamma_L^{\text{AB}}$	$\gamma_L^+$	$\gamma_L^-$	Total surface energy, $\gamma_L$
Distilled water	21.8	51	25.5	25.5	72.8
Ethylene glycol	29	19	1.92	47	48
Methanol	18.2	4.3	0.06	77	22.5
Hexadecane	27.47	0	0	0	27.47

Silicon nitride ( $\text{Si}_3\text{N}_4$ ) ball with 4 mm diameter was used as the counterface material against UHMWPE film in ball-on-disc sliding tests. In order to change the surface energies of the  $\text{Si}_3\text{N}_4$  ball and UHMWPE film, some treatments were given to them. For changing the surface energy of  $\text{Si}_3\text{N}_4$  ball, the air-plasma treatment with 10 min exposure time was given and as another treatment, 3–4 nm thick PFPE film was overcoated onto it. The air-plasma treatment could provide the hydrophilic nature whereas PFPE layer could make the surface hydrophobic. It is difficult to enhance the surface hydrophobicity of  $\text{Si}_3\text{N}_4$  ball only by a physical treatment. That is the reason why PFPE overcoating was chosen as a treatment for hydrophobicity by slightly changing the surface chemistry.

Perfluoropolyether (PFPE) Z-dol 4000 of 0.2 wt% was dissolved into H-Galden ZV60 solvent. Chemical formulae of PFPE and HGalden ZV60 are  $\text{HOCH}_2\text{CF}_2\text{O}-(\text{CF}_2\text{CF}_2\text{O})_p-(\text{CF}_2\text{O})_q-\text{CF}_2\text{CH}_2\text{OH}$  and  $\text{HCF}_2\text{O}-(\text{CF}_2\text{O})_p-(\text{CF}_2\text{CF}_2\text{O})_q-\text{CF}_2\text{H}$ , respectively, where the ratio  $p/q$  is 2/3. The dipping and withdrawal speeds were fixed as mentioned above.

For UHMWPE film, since it has hydrophobic property, we did not attempt to increase its surface hydrophobic property. In this case, UHMWPE film was given the air-plasma treatment with different exposure times (30 s, 5 min and 10 min) in order to change the surface energy by making the surface hydrophilic.

Harrick Plasma Cleaner/Steriliser was used for air-plasma treatment with the different exposure times and a RF power of 30 W under vacuum.

## 2.2 Contact angle measurements and surface energy analysis

After giving different treatments to the samples, their surface energies were determined by the contact angle measurement. The relationship between the contact angle and the surface free energy was first demonstrated by Young with a single droplet on the surface [15]. The Young equation is written in the form

$$\gamma_{sv} = \gamma_{sl} + \gamma_{lv} \cos \theta \quad (1)$$

where  $\theta$  is the contact angle,  $\gamma$  is the surface energy and the subscripts SV, SL and LV represent surface–vapor, surface–liquid and liquid–vapor interfaces, respectively. In determining the surface energy from the contact angle measurement, we used acid–base method [16] in which at least three test liquids are required. In three liquids, at least two have known acid and base fractions larger than zero and at least one must be equal basic and polar parts usually water. In the contact angle measurements in this study, four different liquids: distilled water, ethylene glycol, methanol and hexadecane were used with VCA Optima Contact Angle System (AST product, Inc., USA). The surface tension components and the parameter of the liquids used in this study are provided in Table 1 [17].

Droplets of 0.5  $\mu\text{l}$  and 0.05  $\mu\text{l}$  were used for contact angle measurements of surfaces (UHMWPE film and Si) and  $\text{Si}_3\text{N}_4$  ball, respectively. The droplet size for the measurements on  $\text{Si}_3\text{N}_4$  balls was reduced because of the curvature of the spherical ball. As an additional confirmation of the effect of droplet size (from 0.05  $\mu\text{l}$  to 5  $\mu\text{l}$ ), water contact angles were measured on a flat surface with different droplet sizes and the results did not show any droplet size effect within the given size range. A total of five independent measurements were conducted randomly on three samples and an average value was taken for each sample. The measurement error was within  $\pm 3^\circ$ . After measuring the contact angle with different liquids, the surface energies were calculated using the software installed in the same contact angle equipment. In order to confirm the accuracy of the technique used to determine the surface energy of the samples, PFPE was overcoated on flat Si and UHMWPE film, and then the measured surface energy values were compared with the reported value [18].

The friction between two solid bodies depends not only on the surface energies but also on the surface roughness [19]. Therefore, the roughness of the ball and UHMWPE film were measured before and after surface treatments using dynamic MEMS optical profilers (Veeco Wyko NT100) (a non-contact profiling device). The scanning area for the measurement was 124  $\mu\text{m} \times 93 \mu\text{m}$  on VSI (vertical scan interferometry) mode.

### 2.3 Surface energy and attractive force between surfaces

It is known that when two surfaces (e.g. ball and a flat surface) come into contact, there is finite force acting between them called attractive or pull-off force,  $F_o$ . This force, which depends upon the surface energies of the solids, was first derived by Bradley [20] in 1932 and is given as [19, 20],

$$F_o = 2\pi R(\gamma_1 + \gamma_2 - \gamma_{12}) \quad (2)$$

where  $\gamma_1$  and  $\gamma_2$  are surface energies of the two surfaces and  $\gamma_{12} = (\sqrt{\gamma_1} - \sqrt{\gamma_2})^2$ .

The attractive or pull-off force,  $F_o$  between two different surface energies of the ball and UHMWPE film was calculated using Eq. (2). A detailed calculation procedure of  $F_o$  can be found in Refs. [19, 20].

### 2.4 Friction tests

Friction tests were carefully conducted using a custom-built ball-on-disc tribometer (Fig. 1) where normal and lateral displacements (converted to normal load and friction force, respectively) of the cantilever were simultaneously measured with laser displacement sensors (MTI Instruments Inc., New York, USA). The sensitivity of the laser sensor was 0.5  $\mu\text{m}$  which was equivalent to 0.125 mN force according to our calibrations. UHMWPE film was used as a rotating disc and silicon nitride balls with modified surface energies were used as the stationary counterface. The sliding track radius was 1 mm with a fixed disc rotational speed of 2 rpm (linear relative speed at the contact was in the range of 0.21 mm/s). The sampling rate used in recording data was 10 Hz. In order to eliminate the effect of loading time on friction, the tests were conducted immediately after applying the normal load. The initial coefficient friction was taken as the maximum friction value as soon as the sliding test started. Three repeats of sliding tests on at least three samples were conducted and averages were reported as the final values. The temperature and the relative humidity were fixed at 25  $^\circ\text{C}$  and 65 %, respectively.

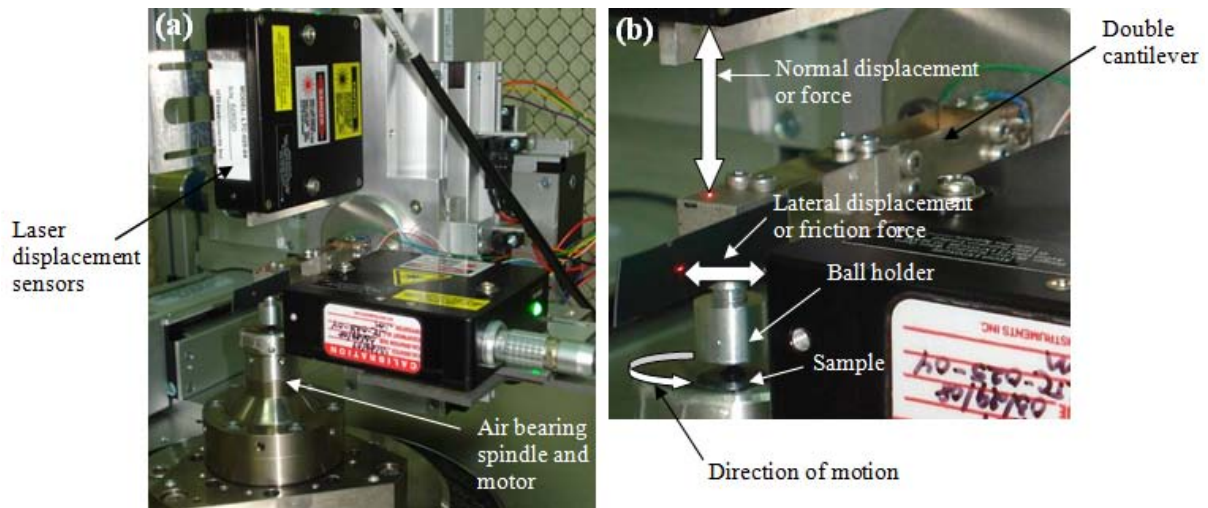


**Fig. 1** (a) Ball-on-disc tribometer, (b) larger view of the cantilever and the sample holder. White arrows indicate the rotational direction of the flat sample and the normal and lateral movement directions of the cantilever.

### 3 Results and discussion

#### 3.1 Surface energy and roughness

The surface treatments, surface energies and roughness of the ball and the surfaces used are summarized in Table 2. The surface energy of PFPE reported in the literature is in the range of 22–24 mJ/m<sup>2</sup> depending upon the concentration and molecular weight [18]. The currently measured values of PFPE layers on Si<sub>3</sub>N<sub>4</sub> ball, Si surface and UHMWPE film are 17.9 mJ/m<sup>2</sup>, 24.13 mJ/m<sup>2</sup> and 23.7 mJ/m<sup>2</sup>, respectively. A slight change in the surface energy of Si<sub>3</sub>N<sub>4</sub> ball may be because of the different measurement conditions between flat surfaces (Si and UHMWPE film) and spherical surface (Si<sub>3</sub>N<sub>4</sub> ball). Except this small deviation, our measured values and the ones provided by the supplier in Ref. [18] are close. It shows that our method of surface energy measurement is reliable.

Though the surface energy of most ceramic materials is very high, the surface energy of silicon nitride ball used in this study is low as evident from the contact angle measurements. Before giving any surface treatment, its contact angle was 83.4°. By giving plasma treatment for 10 min, the contact angle dropped to 38° but it was still measurable. After PFPE overcoating, the contact angle rose to 95.3° in the hydrophobic range. The water contact angle measurement images on Si<sub>3</sub>N<sub>4</sub> balls with different treatments are shown in Fig. 2.

**Table 2.** A summary of surface roughness, treatments and surface energy of silicon nitride ball, UHMWPE film and Si surface. PFPE refers perfluoropolyether (Z-dol 4000) which was coated as 3–4 nm film on the solids mentioned.

Sample	Roughness	Treatment	Surface Energy (mJ/m <sup>2</sup> )			
			Dispersive	Acid	Base	Total
Si <sub>3</sub> N <sub>4</sub> ball ( $\gamma_1$ )	5 nm	PFPE coated	10.5	2.4	5.7	17.9
		No treatment	21	-	24.9	21
		Air Plasma (10 mins)	24.7	0.1	62.5	29.7
UHMWPE coated Si ( $\gamma_2$ )	0.6 $\mu$ m	PFPE coated	23.5	0.1	0.1	23.7
		No treatment	26.9	-	2.6	26.9
		Air Plasma (30s)	27.4	2.5	30.7	44.92
		Air Plasma (5 mins)	27.4	2.9	29.6	45.93
		Air Plasma (10 mins)	27.3	2.4	38.5	46.52
Bare Si ( $\gamma_2$ )	0.41 nm	PFPE coated	13.6	1.9	14.6	24.13

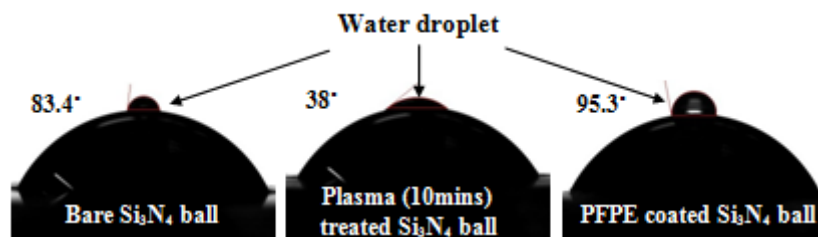


**Fig. 2** The water contact angle measurement on Si<sub>3</sub>N<sub>4</sub> balls with different treatments.

The surface energy of UHMWPE without plasma treatment was 26.9 mJ/m<sup>2</sup>. A increase in the surface energy of UHMWPE was observed by the air-plasma treatment. After 30 s of air-plasma

exposure time, the surface energy rose to 44.92 mJ/m<sup>2</sup>. This value did not change further in any significant way with increasing exposure time to 5 min and 10 min.

The measured roughness value on Si<sub>3</sub>N<sub>4</sub> ball and UHMWPE film were 5 nm and 0.6 μm, respectively. Negligible differences in the surface roughness were observed in the cases of Si<sub>3</sub>N<sub>4</sub> ball and UHMWPE film after air-plasma or PFPE treatments. Therefore, the effect of surface roughness on the measured surface energies was neglected. Also, the surface roughness did not vary within one single friction test. The effect of interfacial temperature was also neglected as the friction tests were conducted at very low sliding speeds in a temperature controlled environment.

Based on the surface energy of Si<sub>3</sub>N<sub>4</sub> ball and UHMWPE film with different treatments, the attractive force,  $F_o$  was calculated using Eq. (2). The calculated attractive forces between different surface pairs are shown in Table 3.

**Table 3.** The attractive force,  $F_o$  between Si<sub>3</sub>N<sub>4</sub> ball and UHMWPE film with different surface energies.

Si <sub>3</sub> N <sub>4</sub> Ball ( $\gamma_1$ )		UHMWPE film ( $\gamma_2$ )		$F_o$ (mJ/m <sup>2</sup> )
Treatment	Surface Energy (mJ/m <sup>2</sup> )	Treatment	Surface Energy (mJ/m <sup>2</sup> )	
PFPE coated	17.9	No treatment	26.9	0.55
No treatment	21	Air Plasma (10 mins)	46.52	0.79
Air Plasma (10 mins)	29.7	No treatment	26.9	0.71
PFPE coated	17.9	Air Plasma (10 mins)	46.52	0.72
No treatment	21	No treatment	26.9	0.6
Air Plasma (10 mins)	29.7	Air Plasma (10 mins)	46.52	0.93

### 3.2 The relationship between the initial shear stress and the surface energy on UHMWPE film

The friction tests were conducted using the different pairs of Si<sub>3</sub>N<sub>4</sub> ball and UHMWPE film mentioned in Table 3, and the shear stress,  $\tau$  was calculated by dividing the measured friction force with the contact area [9, 21]. In order to obtain the contact area between the ball and UHMWPE film, JKR model (Eq. (3)) was applied in which the effect of surface energy is taken into account.

$$a^3 = \frac{R}{K} \left( L + 3\pi R + \sqrt{6\pi RL + \frac{4}{3}\pi R} \right)^2 \quad (3)$$

where  $a$  is the contact radius,  $R$  is the sphere radius,  $K$  depends on the Poisson's ratio and elastic modulus of the materials,  $L$  is the applied load and  $\gamma$  is the surface energy. The Poisson's ratios and elastic moduli of the materials used are provided in Table 4. The contact pressure,  $P$  was calculated by dividing the applied normal loads with the contact area,  $\pi a^2$ . By varying the applied normal load from 15 mN to 75 mN, the calculated contact pressure is varied from 59 MPa to 117 MPa for the mentioned contacting surfaces.

After obtaining the shear stress,  $\tau$  and the contact pressure,  $P$  for different  $F_o$  (varying from 0.55 mN to 0.93 mN) between the ball and UHMWPE film, we plotted them as shown in Fig. 3. It is seen that  $\tau$  increases linearly with increasing  $P$  although the magnitude of  $\tau$  is strongly influenced by the attractive force,  $F_o$  (that is the adhesive interactions between the surfaces). It is well noted that higher  $F_o$  provides higher  $\tau$ . The data also confirms the linear relation  $\tau = \tau_o + \alpha P$  as proposed by Bowden and

Tabor [22] where the pressure coefficient,  $\alpha = 0.0013$ , same for all  $F_0$ . However, the normal pressure-independent initial shear stress,  $\tau_0$  increases as  $F_0$  is increased within the range of presently applied loads. Robbins et al. [23–26] have also shown by molecular dynamic simulation that  $\tau_0$  increases as adhesion or attractive force is increased whereas  $\alpha$  does not change.  $\tau_0$  is the initial shear stress when the contact pressure,  $P = 0$ .

**Table 4.** The Poisson’s ratio and elastic modulus for silicon nitride ball and UHMWPE film.

Material	Poisson’s ratio	Elastic modulus (GPa)
Silicon nitride ball	0.22	310
UHMWPE film	0.46	1

Adhesion between contacting solids at rest is partially transformed into elastic strain in the cantilever at the onset of lateral sliding motion. The stored elastic energy in the cantilever will be released when the friction force in the lateral direction is more than the combined stiffness of the cantilever and the contact [27]. This is the point at which the actual sliding starts giving the lateral force at release (or slip) as the initial friction.  $\tau_0$  is an important parameter controlling initial friction which changes with the pull-off force,  $F_0$ . Fig. 4 presents the data for  $F_0$  and  $\tau_0$  for  $\text{Si}_3\text{N}_4$  ball and UHMWPE film. It is evident that  $\tau_0$  increases slightly with  $F_0$  up to 0.72 mN and beyond this value,  $\tau_0$  rises abruptly. As we mentioned before, the application of PFPE could affect the frictional behavior of UHMWPE film. It could help to lower the friction in addition to lowering the surface energy. However, when the data of PFPE are removed from Fig. 4(a), it is obvious that the relationship between  $F_0$  and  $\tau_0$  is still an exponential curve (see in Fig. 4(b)) with only slight changes in the curve fitting parameters. Thus, this behavior between  $F_0$  and  $\tau_0$  can be modeled by an exponential curve of the following form,

$$\tau_0 = c_1 \exp(n F_0) \tag{4}$$

where  $c_1$  and  $n$  are constants that depend upon the nature of the surface materials. The values of  $c_1$  and  $n$  shown in Fig. 4 (a) are  $9 \times 10^{-5}$  MPa and  $8.4 \text{ (mN)}^{-1}$ , respectively.

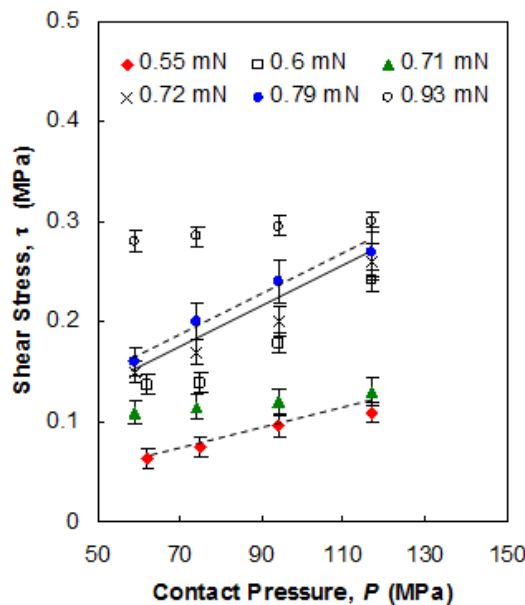


**Fig. 3** Shear stress versus contact pressure on UHMWPE film. All attractive or pull off forces,  $F_0$  show linearly increasing trend with shear stress, as contact pressure is increased.

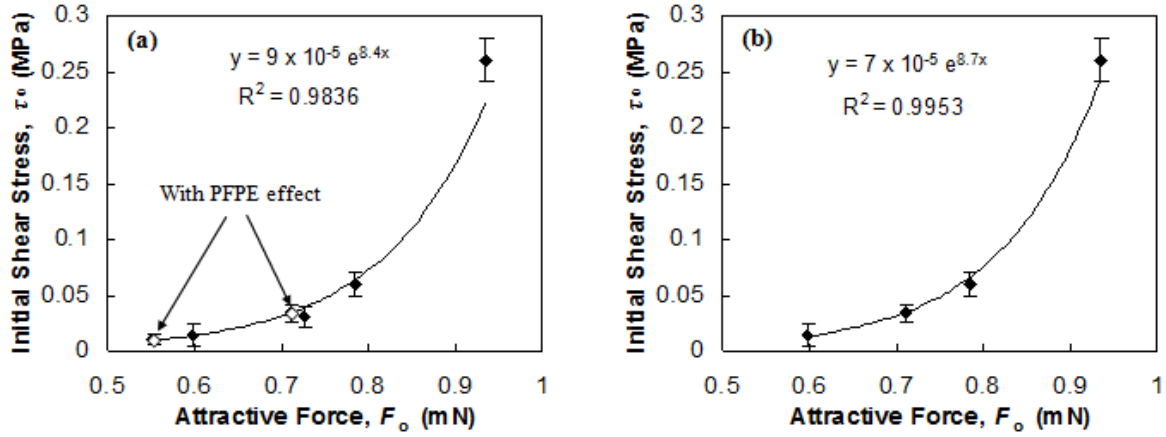


Fig. 4 The initial shear stress,  $\tau_0$  as a function of the attractive force,  $F_0$  of UHMWPE film (a) with PFPE effect and (b) without PFPE effect. There is an exponential relation between the two.

### 3.3 Relation between initial coefficient of friction and surface energy on UHMWPE film

Since  $\tau = \tau_0 + \alpha P$  and the initial friction force,  $F_i = \tau A$ , we can write as

$$F_i = \tau_0 A + \alpha P A \quad (5)$$

By dividing Eq. (5) with applied load,  $L$ , we obtain the initial coefficient of friction,  $\mu_i$  as

$$\mu_i = \left[ \frac{\tau_0}{L} \times A \right] + \alpha \quad (6)$$

where  $P = L/A$ . Finally, we can correlate  $\mu_i$  as a function of attractive or pull-off force,  $F_0$  using Eqs. (4) and (6) as

$$\mu_i = \left[ \frac{c_1 \exp(nF_0)}{L} \times A \right] + \alpha \quad (7)$$

For the visco-elastic materials such as UHMWPE film, Bowden and Tabor [28] suggested that the contact area,  $A$  is nearly proportional to  $L^{0.75}$ . Since  $A = c_2 L^{0.75}$  where  $c_2$  is a constant equal to  $0.74 \pm 0.18 \text{ m}^2 \text{ N}^{-0.75}$ , Eq. (7) then becomes,

$$\mu_i = \left[ \frac{c_1 c_2 \exp(nF_0)}{L^{0.25}} \right] + \alpha \quad (8)$$

In order to verify this relationship, we measured  $\mu_i$  at different  $F_0$  (using two additional  $F_0$  at 0.77 mN and 0.78 mN) on UHMWPE film for different normal applied loads. In Fig. 5, the curves show a very similar exponential relation between  $\mu_i$  and  $F_0$  for different applied loads and variations are within experimental errors. In addition, it might be assumed that the highest frictional value at 0.93mN ( $F_0$ ) (which represents the ball and UHMWPE film that were given 10 min plasma treatment) has additional effect of covalent bonding between oxygen species that were introduced onto the ball and UHMWPE

film due to air-plasma treatment. Despite some chemical effects, we observe that the relation between the initial coefficient of friction and the pull-off force due to surface energy is of exponential type.

Similar exponential trend has been shown by Erhard [29] and Lavielle [30]. They studied friction between different polymers with different surface energies (55–90 mJ/m<sup>2</sup>) and found that the coefficient of friction was exponential to the surface energies of the sliding polymers. In the present study, we have used a fixed polymer film (UHMWPE) with modified surface energies and similar exponential relation is observed. Another interesting behavior we have seen from this study is that  $\mu_i$  drops with increasing load (Fig. 5 (a) and (b)) as predicted by Eq. (8) within the load range adopted here.

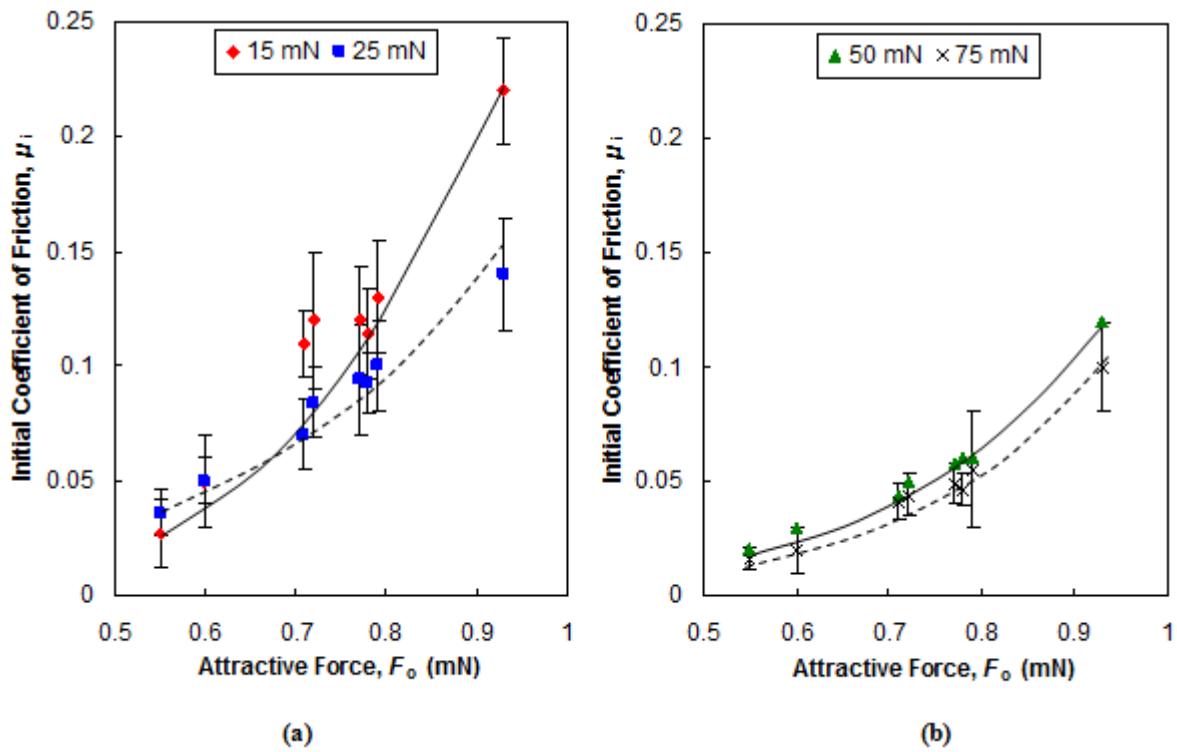
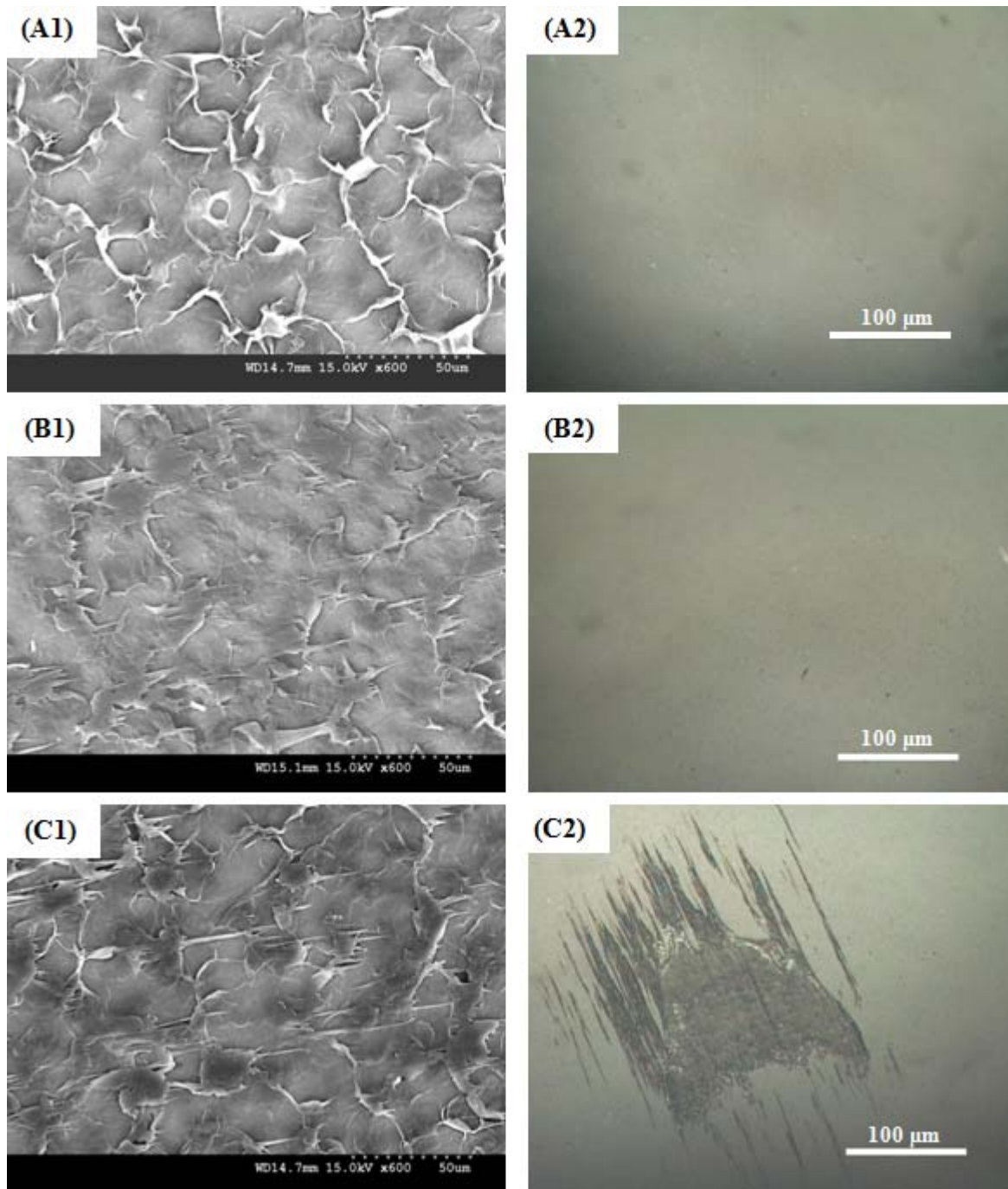


Fig. 5 The initial coefficient of friction of UHMWPE film versus  $F_o$  for different applied loads: (a) low loads and (b) higher loads.



**Fig. 6** Figure (A<sub>1</sub>) and (A<sub>2</sub>) are FESEM image of UHMWPE film and optical image of Si<sub>3</sub>N<sub>4</sub> ball before experiment, respectively. (B<sub>1</sub>) and (C<sub>1</sub>) are FESEM images of UHMWPE films after sliding against (B<sub>2</sub>) PFPE coated Si<sub>3</sub>N<sub>4</sub> and (C<sub>2</sub>) bare Si<sub>3</sub>N<sub>4</sub> balls, respectively, where the applied load is 15 mN.

### 3.4 Material transfer between UHMWPE film and different surface energy balls

The tracks on UHMWPE films after two cycles of sliding against PFPE coated Si<sub>3</sub>N<sub>4</sub> and untreated Si<sub>3</sub>N<sub>4</sub> balls are shown in Fig. 6 (B<sub>1</sub> and C<sub>1</sub>), respectively. The tests were conducted under an applied load of 15mN and a rotational speed of 2 rpm. The track on UHMWPE film, which was slid against low surface energy (PFPE coated) ball, shows some orientation of the polymer asperities made by the ball surface. Because of the low adhesion between UHMWPE film and PFPE coated ball, the probability of materials being pulled out, plastically deformed or scratched is very less. After the sliding test, the optical images of the ball surface were taken under an optical microscope. From the image, it is

obvious that the amount of material transferred to PFPE coated ball was very less if any (Fig. 6 (B2)). However when UHMWPE film was slid against high surface energy (untreated) ball, the track shows discontinuous scratches. It proves that high surface energy ball provides strong adhesion and as a result polymer is pulled out. The discontinuous nature of the scratch marks on the track suggests the effect of high surface energy in material removal of the counterface rather than scratching by the asperities on the ball surface which is very smooth (5 nm roughness).

It is also clear in the optical image (Fig. 6 (C2)) that lumps of polymer transfer easily to the ball surface when the surface energy of the ball is high. The microscopic images show the differences in the shear mechanisms when surfaces with different surface energies are involved. This basically governs the materials' wear characteristics.

#### 4 Conclusion

In summary, we have studied the shear stress,  $\tau$ , with the contact pressure,  $P$  on UHMWPE film in conjunction with the effect of attractive or pull-off force,  $F_o$ . Data show that  $\tau$  increases linearly with increasing  $P$  as proposed by Bowden and Tabor whereas the pressure-independent initial shear stress,  $\tau_o$  increases exponentially with  $F_o$ . Based on the trends between  $\tau_o$  and  $F_o$  from the experimental data, an exponential relation is proposed. According to this model, the initial coefficient of friction,  $\tau_i$ , increases exponentially with increasing  $F_o$ . Further,  $\tau_i$  shows a decreasing trend with increasing applied load,  $L$ , at a given  $F_o$  for polymer surface because of its visco-elastic nature.

Since the attractive force is directly proportional to the surface energy (Eq. (2)), we can control friction by modifying the energies of the solids involved. This study will provide a better understanding of the initial friction and nanolubrication in small devices such as MEMS/NEMS where the surface energy of small moving parts can be easily changed and controlled. Surface energy is also directly responsible for the removal of the polymer material as wear debris.

#### Acknowledgements

This project was financially supported by a research grant from the Faculty of Engineering, NUS (#R-265-000-248-112). One of the authors (MM) would like to acknowledge the Graduate School of Engineering, NUS, for the scholarship awarded to support his studies at NUS.

## References

1. D. Dowson, *History of Tribology*, Longman, London and New York, 1979.
2. K.L. Johnson, K. Kendall, A.D. Roberts, *Proc. R. Soc. Lond. Ser. A* 324 (1971) 01.
3. B.V. Derjaguin, V.M. Muller, Y.P. Toporov, *J. Colloid Interface Sci.* 53 (1975) 314.
4. J.N. Israelachvili, D. Tabor, *Proc. R. Soc. Lond. Ser. A* 331 (1972) 19.
5. H. Yoshizawa, Y.-L. Chen, J.N. Israelachvili, *J. Phys. Chem.* 97 (1993) 4128.
6. A.D. Corwin, M.P. de Boer, *Appl. Phys. Lett.* 84 (2004) 2451.
7. N. Maeda, N. Chen, M. Tirrell, J.N. Israelachvili, *Science* 297 (2002) 379.
8. L. Lee, *Recent Advances in Polymer Friction and Wear*, Gordon and Breach, New York, 1974.
9. B.J. Briscoe, D. Tabor, *J. Adhes.* 9 (1978) 145.
10. B.J. Briscoe, D. Tabor, in: D. Clark, D. Feast (Eds.), *Friction and Wear of Polymers in Surface Properties*, Plenum, London, 1978.
11. B.J. Briscoe, in: D. Clark, D. Feast (Eds.), *Adhesion of Elastomers in Surface Properties of Polymers*, Plenum, London, 1978.
12. G.W. Tyndall, P.B. Leezenberg, *Trib. Lett.* 4 (1998) 103.
13. M. Yanagisawa, *Tribology and Mechanics of Magnetic Storage Systems*, STLE SP-19, vol. II, 1985, p. 16.
14. H. Tian, T. Matsudaira, *ASME J. Trib.* 115 (1993) 28.
15. T. Young, in: G. Peacock (Ed.), *Miscellaneous Works*, vol. 1, Murray, London, 1855, p. 418.
16. C.J. van Oss, *Interfacial Force in Aqueous Media*, Marcel Dekker, New York, 1994, pp. 20-21.
17. C.J. van Oss, *Interfacial Force in Aqueous Media*, Marcel Dekker, New York, 1994, pp. 171-75.
18. Website: [http://www.solvaysolexis.com/static/wma/pdf/5/4/3/4/fom\\_thin.pdf](http://www.solvaysolexis.com/static/wma/pdf/5/4/3/4/fom_thin.pdf) last accessed in July 2009.
19. D. Tabor, *J. Colloid Interface Sci.* 58 (1977) 2.
20. R.S. Bradley, *Philos. Mag.* 13 (1932) 583.
21. B.J. Briscoe, B. Scruton, R.F. Willis, *Proc. R. Soc. Lond. Ser. A* 333 (1973) 99.
22. F.P. Bowden, D. Tabor, *The Friction and Lubrication of Solids*, Oxford University Press, Oxford, 1958.
23. G. He, M.H. Müser, M.O. Robbins, *Science* 284 (1999) 1650.
24. G. He, M.O. Robbins, *Phys. Rev. B* 64 (2001) 035413.
25. H.M. Müser, L. Wenning, M.O. Robbins, *Phys. Rev. Lett.* 86 (2001) 1295.
26. J. Rottler, M.O. Robbins, *Phys. Rev. E* 64 (2001) 051801.
27. R.W. Carpick, *Science* 313 (2006) 184.
28. F.P. Bowden, D. Tabor, *Friction: An Introduction to Tribology*, Anchor Press, New York, 1973.
29. G. Erhard, *Wear* 84 (1983) 167.
30. L. Lavielle, *Wear* 151 (1991) 63.